# Stress analysis of functionally graded plates with different gradient direction †\*M. Amirpour¹, R. Das¹, and E.I. Saavedra Flores²

<sup>1</sup>Department of Mechanical Engineering, University of Auckland, Auckland 1010, New Zealand <sup>2</sup> Departamento de Ingeniería en Obras Civiles, Universidad de Santiago de Chile, Av. Ecuador 3659, Santiago, Chile

\*Presenting author: maedeh.amirpourmolla@auckland.ac.nz †Corresponding author: maedeh.amirpourmolla @auckland.ac.nz

## Abstract

The purpose of this paper is to investigate the general deformation pattern and stress field of a thin rectangular FGM plate for different property gradient directions, i.e. perpendicular and parallel to the loading direction, both analytically and numerically. The relevant governing equations of elasticity are solved with static analysis with power law distribution of volume fraction of constituents, and the analytical solutions for the displacements and stresses are derived. The resultant solutions are verified against numerical solutions obtained using the finite element method (FEM). The finite element (FE) solution is obtained using solid elements with spatially graded property distribution (at different gauss points), which is implemented by a user material subroutine (UMAT) in the ABAQUS FE software. The obtained results demonstrate that the direction of material property gradient and the nature of its variation have significant effects on the mechanical behavior of FGM plates. Moreover, the comparison between the exact solution and numerical simulation shows the efficiency of graded solid elements in modelling of thin FGM plate. Keywords: FGM, stress field, power-law distribution, finite element method, elasticity, graded solid elements.

#### Introduction

Functionally Graded Materials (FGMs) are advanced engineered materials whereby material composition and properties vary spatially in macroscopic length scales, which are created by specialized manufacturing processes. The main advantage of FGMs is the elimination of stress concentration and discontinuity in the interface due to the monotonous variation of volume fraction of the constituents. There are various mathematical models to describe distribution of volume fraction of constituents, i.e. power- law and exponential law. Some researchers used exponential function for defining material property variation (Guo & Noda, 2014; Z. Wang, Guo, & Zhang, 2013). Another form of mathematical model using a power-law distribution has been widely used in a number of studies, especially for the mechanical engineering field (Cheng & Batra, 2000; Navazi, Haddadpour, & Rasekh, 2006; Sun & Luo, 2011). There are a significant growth in literatures corresponding to FGMs in the mechanics of FGMs (Chi & Chung, 2006; Thai & Choi, 2013; C. Wang & Xu, 2014), manufacture process (El-Desouky, Kassegneb, Moonb, McKittrickc, & Morsib, 2013; Kieback, Neubrand, & Riedel, 2003), crack growth and damage (Bocciarelli, Bolzon, & Maier, 2008; Eghtesad, Shafiei, & Mahzoon, 2012; Torshizian & Kargarnovin, 2014) in last 10 years.

One of the wide applications of FGM is in plate structures as thermal barriers. Therefore, understanding the mechanical behavior of an FGM plate is vital for

effective design of structures employing FGMs to meet desired and safety criteria. An exact solution for exponentially graded FGM plates with simply-supported boundary condition under a surface load was expanded by Pan (Pan, 2003). Further, Chi (Chi & Chung, 2006) derived an analytical formulation for three types of distribution function namely power-law, sigmoid and exponential based on classical plate theory (CPT) for rectangle simply supported FGM plate with transverse loading. They evaluated the exact solution with numerical simulation by MARC FE program with 16 layers of different material properties in thickness direction. Recently, (Akbarzadeh, Hosseini zad, Eslami, & Sadighi, 2010) used the first-order shear deformation theory (FSDT) and the third-order shear deformation theory (TSDT) for FGM plate with the power- law distribution of the volume fraction. They obtained the natural frequencies and dynamic responses of the FGM plate analytically. All the mentioned studies have been carried out with regards to variation of material constituents through the thickness. However, no studies are known on distribution of volume fraction through the length of the plate.

During manufacturing process of FGMs, the reliability requirements for the product should be considered to meet desired or application-specific performance criteria. One approach to produce FGMs is use of additive manufacturing (3D printing), which can control local composition and microstructure. Furthermore, the gradient distribution and its relationship with the loading direction will affect the macro stiffness and mechanical behavior.

This paper presents the behavior of the thin rectangular FGM plate with CPT assumptions under transverse loading. The close forms solutions based on Fourier series expression for power- law distributions in two different gradient directions (the thickness direction and length direction) are obtained. Moreover, the analytical solutions are proved by the numerical simulation of the finite element method using ABAQUS. In numerical modelling, the graded solid elements are implemented in the user material subroutine (UMAT). These results will possibly enable us to understand the behavior of new materials with controlled macro properties.

## **Analytical Solutions**

## State I- Gradient distribution in thickness direction

Let us consider an elastic rectangular plate. As shown in Fig. 1a, coordinates x and y define the plane of the plate, whereas the z-axis originated at the middle surface of the plate is in the thickness direction. The Poisson ratio is assumed to be constant. However, the Young's moduli in thickness direction vary with Eq. (1) and the elastic modulus can be determined by the rule of mixture:

$$V_{i}(z) = (\frac{1}{2} + \frac{z}{h})^{n} \tag{1}$$

$$E(z) = V_i(z)E_i + (1 - V_i(z))E_m = \left(\frac{1}{2} + \frac{z}{h}\right)^n (E_i - E_m) + E_m$$
 (2)

Where n is the power-law index, h is the thickness of the plate,  $E_i$  and  $E_m$  are the Young's moduli of inclusion and matrix, respectively.

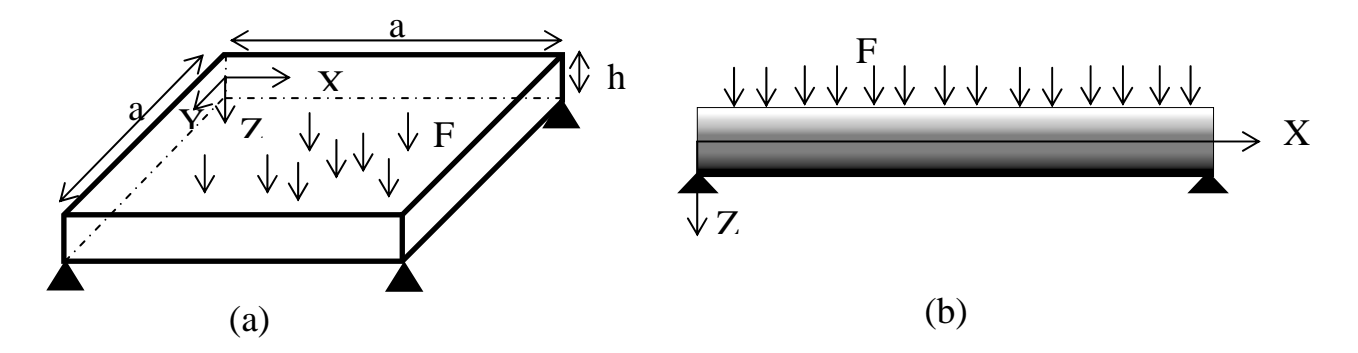


Figure 1. a) The Geometry of FGM Plate. b) The distribution of volume fraction in Z direction:  $V_i(z) = (\frac{1}{2} + \frac{z}{h})^n$ 

It is assumed that the deformations and the stresses of the thin FGM plate are based upon classical plate theory. So, the strain and stress fields are:

$$\varepsilon_{x} = \varepsilon_{x0} - z \frac{\partial^{2} w}{\partial x^{2}} \tag{3a}$$

$$\varepsilon_{y} = \varepsilon_{y0} - z \frac{\partial^{2} w}{\partial y^{2}} \tag{3b}$$

$$\gamma_{xy} = \gamma_{xy0} - 2z \frac{\partial^2 w}{\partial x \partial y}$$
 (3c)

$$\sigma_{x} = \frac{E(z)}{1 - v^{2}} \left[ \varepsilon_{x0} + v \varepsilon_{y0} - z \frac{\partial^{2} w}{\partial x^{2}} - v z \frac{\partial^{2} w}{\partial y^{2}} \right]$$
(3d)

$$\sigma_{y} = \frac{E(z)}{1 - v^{2}} \left[ \varepsilon_{y0} + v \varepsilon_{x0} - z \frac{\partial^{2} w}{\partial y^{2}} - v z \frac{\partial^{2} w}{\partial x^{2}} \right]$$
 (3e)

$$\tau_{xy} = \frac{E(z)}{1 - v^2} \frac{1 - v}{2} \left[ \gamma_{xy0} - 2z \frac{\partial^2 w}{\partial x \partial y} \right]$$
 (3f)

In this work, the thickness of thin plate is assumed to be in the range  $1/20 \sim 1/100$  of its length. So, the transverse shear deformations should be eliminated.

The matrix formation of axial forces and momentum are:

$$\begin{pmatrix}
N_{x} \\
N_{y} \\
N_{xy}
\end{pmatrix} = \begin{bmatrix}
A_{11} & A_{12} & 0 \\
A_{12} & A_{11} & 0 \\
0 & 0 & A_{66}
\end{bmatrix}
\begin{pmatrix}
\varepsilon_{x0} \\
\varepsilon_{y0} \\
\gamma_{xy0}
\end{pmatrix} + \begin{bmatrix}
B_{11} & B_{12} & 0 \\
B_{12} & B_{11} & 0 \\
0 & 0 & B_{66}
\end{bmatrix}
\begin{pmatrix}
-\frac{\partial^{2} w}{\partial x^{2}} \\
-\frac{\partial^{2} w}{\partial y^{2}} \\
-2\frac{\partial^{2} w}{\partial x \partial y}
\end{pmatrix}$$
(4a)

$$\begin{pmatrix} M_{x} \\ M_{y} \\ M_{xy} \end{pmatrix} = \begin{bmatrix} B_{11} & B_{12} & 0 \\ B_{12} & B_{11} & 0 \\ 0 & 0 & B_{66} \end{bmatrix} \begin{pmatrix} \varepsilon_{x0} \\ \varepsilon_{y0} \\ \gamma_{xy0} \end{pmatrix} + \begin{bmatrix} C_{11} & C_{12} & 0 \\ C_{12} & C_{11} & 0 \\ 0 & 0 & C_{66} \end{bmatrix} \begin{pmatrix} -\frac{\partial^{2} w}{\partial x^{2}} \\ -\frac{\partial^{2} w}{\partial y^{2}} \\ -2\frac{\partial^{2} w}{\partial x \partial y} \end{pmatrix}$$
(4b)

The coefficients of above equations are depending on the material properties of FGM plate. So, for the above rectangular FGM plate we have:

$$A_{11} = \int_{-h/2}^{h/2} \frac{E(z)}{1 - v^2} dz = \int_{-h/2}^{h/2} \frac{1}{2} + \frac{z}{h} \int_{1-v^2}^{n} (E_i - E_m) + E_m dz = \frac{h}{1 - v^2} \frac{(nE_m + E_i)}{n + 1}$$

$$A_{12} = vA_{11} = \frac{vh}{1 - v^2} \frac{(nE_m + E_i)}{n + 1}$$

$$A_{66} = \frac{1 - v}{2} A_{11} = \frac{1 - v}{2} \frac{h}{1 - v^2} \frac{(nE_m + E_i)}{n + 1}$$

$$B_{11} = \int_{-h/2}^{h/2} \frac{zE(z)}{1 - v^2} dz = \frac{1}{1 - v^2} \int_{-h/2}^{h/2} z \left( \frac{1}{2} + \frac{z}{h} \right)^n (E_i - E_m) + zE_m dz = \frac{h^2}{1 - v^2} \frac{n(E_i - E_m)}{2(n + 1)(n + 2)}$$

$$B_{12} = vB_{11} = \frac{vh^2}{1 - v^2} \frac{n(E_i - E_m)}{2(n + 1)(n + 2)}$$

$$C_{11} = \int_{-h/2}^{h/2} \frac{z^2E(z)}{1 - v^2} dz = \frac{1}{1 - v^2} \int_{-h/2}^{h/2} z^2 \left( \frac{1}{2} + \frac{z}{h} \right)^n (E_i - E_m) + E_m dz = \frac{h^3}{12(1 - v^2)} \left( \frac{3(n^2 + n + 2)(E_i - E_m)}{(n + 1)(n + 2)(n + 3)} + E_m \right)$$

$$C_{12} = vC_{11} = \frac{vh^3}{12(1 - v^2)} \left( \frac{3(n^2 + n + 2)(E_i - E_m)}{(n + 1)(n + 2)(n + 3)} + E_m \right)$$

$$C_{66} = \frac{1 - v}{2} C_{11} = \frac{1 - v}{2} \frac{h^3}{12(1 - v^2)} \left( \frac{3(n^2 + n + 2)(E_i - E_m)}{(n + 1)(n + 2)(n + 3)} + E_m \right)$$

$$(5c)$$

With definition of the uniform distributed transverse loading by Fourier series, the equilibrium equation can be written as:

$$\frac{\partial^2 M_x}{\partial x^2} + \frac{\partial^2 M_y}{\partial y^2} + 2 \frac{\partial^2 M_{xy}}{\partial x \partial y} = -F = -\sum \sum F_{mn} \sin \frac{m\pi x}{a} \sin \frac{n\pi y}{a}$$

$$F_{mn} = \begin{cases}
\frac{16F}{\pi^2 mn} & n, m = 1, 3, 5, \dots \\
0 & n, m = 2, 4, 6, \dots
\end{cases}$$
(6)

With definition of stress function  $\Phi(x, y)$  and  $N_x = \frac{\partial^2 \Phi}{\partial y^2}$ ,  $N_y = \frac{\partial^2 \Phi}{\partial x^2}$ ,  $N_{xy} = \frac{\partial^2 \Phi}{\partial x \partial y}$ , the strains at the middle surface are expressed in terms of the stress function and the deflection:

$$\begin{pmatrix}
\varepsilon_{x0} \\
\varepsilon_{y0} \\
\gamma_{xy0}
\end{pmatrix} = \begin{bmatrix}
D_{11} & D_{12} & 0 \\
D_{12} & D_{11} & 0 \\
0 & 0 & D_{66}
\end{bmatrix} \begin{pmatrix}
\frac{\partial^{2}\Phi}{\partial y^{2}} \\
\frac{\partial^{2}\Phi}{\partial x^{2}} \\
\frac{\partial^{2}\Phi}{\partial x\partial y}
\end{pmatrix} + \begin{bmatrix}
E_{11} & E_{12} & 0 \\
E_{12} & E_{11} & 0 \\
0 & 0 & E_{66}
\end{bmatrix} \begin{pmatrix}
-\frac{\partial^{2}w}{\partial x^{2}} \\
-\frac{\partial^{2}w}{\partial y^{2}} \\
-2\frac{\partial^{2}w}{\partial x\partial y}
\end{pmatrix}$$
(7a)

$$\begin{pmatrix} M_{x} \\ M_{y} \\ M_{xy} \end{pmatrix} = -\begin{bmatrix} E_{11} & E_{12} & 0 \\ E_{12} & E_{11} & 0 \\ 0 & 0 & E_{66} \end{bmatrix} \begin{pmatrix} \varepsilon_{x0} \\ \varepsilon_{y0} \\ \gamma_{xy0} \end{pmatrix} + \begin{bmatrix} F_{11} & F_{12} & 0 \\ F_{12} & F_{11} & 0 \\ 0 & 0 & F_{66} \end{bmatrix} \begin{pmatrix} -\frac{\partial^{2} w}{\partial x^{2}} \\ -\frac{\partial^{2} w}{\partial y^{2}} \\ -2\frac{\partial^{2} w}{\partial x \partial y} \end{pmatrix}$$
(7b)

where:

$$D_{11} = \frac{A_{11}}{A_{11}^{2} - A_{12}^{2}} = \frac{1}{1 - v^{2} A_{11}} = \frac{n + 1}{h(nE_{m} + E_{i})}$$

$$D_{12} = \frac{-A_{12}}{A_{11}^{2} - A_{12}^{2}} = \frac{-v A_{11}}{A_{11}^{2} - v^{2} A_{11}^{2}} = \frac{-v(n + 1)}{h(nE_{m} + E_{i})}$$

$$D_{66} = \frac{-1}{A_{66}} = -\frac{2}{1 - v} \frac{1 - v^{2}}{h} \frac{(n + 1)}{(nE_{m} + E_{i})}$$

$$v B_{12} = A_{11} B_{12} - v^{2} A_{12} B_{12} - A_{12} B_{13} - A_{13} B_{14} - A_{14} B_{14} - A_{15} B_{15} - A_$$

$$E_{11} = \frac{A_{12}B_{12} - A_{11}B_{11}}{A_{11}^{2} - A_{12}^{2}} = \frac{v^{2}A_{11}B_{11} - A_{11}B_{11}}{A_{11}^{2} - v^{2}A_{11}^{2}} = -\frac{hn(E_{i} - E_{m})}{2(n+2)(nE_{m} + E_{i})}$$

$$E_{12} = \frac{A_{12}B_{11} - A_{11}B_{12}}{A_{11}^{2} - A_{12}^{2}} = 0$$

$$E_{66} = -\frac{B_{66}}{A_{66}} = -\frac{B_{11}}{A_{11}} = -\frac{hn(E_{i} - E_{m})}{2(n+2)(nE_{m} + E_{i})}$$
(8b)

$$F_{11} = B_{11}E_{11} + B_{12}E_{12} + C_{11} = \frac{h^2}{1 - v^2} \left( \frac{n(E_i - E_m)}{2(n+1)(n+2)} \right) \left( -\frac{hn(E_i - E_m)}{2(n+2)(nE_m + E_i)} \right) + \frac{h^3}{12(1 - v^2)} \left( \frac{3(n^2 + n + 2)(E_i - E_m)}{(n+1)(n+2)(n+3)} + E_m \right)$$

$$F_{12} = vF_{11}$$

$$F_{66} = C_{66} + B_{66}E_{66}$$
(8c)

In order to find the relation between stress function and deflection, we substitute the Eqs. (7a) and (7b) in Eq. (6):

$$E_{12} \frac{\partial^4 \Phi}{\partial x^4} + E_{12} \frac{\partial^4 \Phi}{\partial y^4} + 2(E_{11} - E_{66}) \frac{\partial^4 \Phi}{\partial x^2 \partial y^2} + F_{11} \frac{\partial^4 w}{\partial x^4} + F_{11} \frac{\partial^4 w}{\partial y^4} + 2(F_{12} + 2F_{66}) \frac{\partial^4 w}{\partial x^2 \partial y^2} =$$

$$\sum \sum F_{mn} \sin \frac{m\pi x}{a} \sin \frac{n\pi y}{a}$$

$$(9)$$

A compatibility equation is then used to provide another governing equation. By using Eq. (7a), the compatibility equation

$$\frac{\partial^2 \varepsilon_x}{\partial y^2} + \frac{\partial^2 \varepsilon_y}{\partial x^2} = \frac{\partial^2 \gamma_{xy}}{\partial y \partial x}$$
 (10)

Can be expressed as:

$$D_{11} \frac{\partial^4 \Phi}{\partial x^4} + D_{11} \frac{\partial^4 \Phi}{\partial y^4} + 2(D_{12} - D_{66}) \frac{\partial^4 \Phi}{\partial x^2 \partial y^2} - E_{12} \frac{\partial^4 w}{\partial x^4} - E_{12} \frac{\partial^4 w}{\partial y^4} - 2(E_{11} - E_{66}) \frac{\partial^4 w}{\partial x^2 \partial y^2} = 0 \quad (11)$$

The stress function and deflection can be obtained by simultaneous solution of Eqs. (9) and (11). With definition of Fourier serious for  $\Phi(x, y)$  and w alongside

simultaneous solution of Eqs. (9) and (11), the stress function and deflection can be obtained.

$$w(x,y) = \sum \sum w_{mn} \sin \frac{m\pi x}{a} \sin \frac{m\pi y}{a}$$

$$\Phi(x,y) = \sum \sum \Phi_{mn} \sin \frac{m\pi x}{a} \sin \frac{m\pi y}{a}$$
(12)

where

$$w_{mn} = \left(\frac{1}{F_{11} \left(\left(\frac{m\pi}{a}\right)^2 + \left(\frac{n\pi}{a}\right)^2\right)^2}\right) F_{mn}$$

 $\Phi_{mn} = 0$ 

So, the stress and strain fields for the rectangular FGM plate with the material gradation in thickness direction are:

$$\varepsilon_{x} = \frac{E_{11} + z}{F_{11}} \sum \sum \frac{F_{mm} \left(\frac{m\pi}{a}\right)^{2}}{\left(\left(\frac{m\pi}{a}\right)^{2} + \left(\frac{n\pi}{a}\right)^{2}\right)^{2}} \sin \frac{m\pi x}{a} \sin \frac{m\pi y}{a}$$
(13a)

$$\varepsilon_{y} = \frac{E_{11} + z}{F_{11}} \sum \sum \frac{F_{mn} \left(\frac{n\pi}{a}\right)^{2}}{\left(\left(\frac{m\pi}{a}\right)^{2} + \left(\frac{n\pi}{a}\right)^{2}\right)^{2}} \sin \frac{m\pi x}{a} \sin \frac{m\pi y}{a}$$
(13b)

$$\gamma_{xy} = \frac{-2(E_{11} + z)}{F_{11}} \sum \sum \frac{F_{mn} \left(\frac{n\pi}{a}\right) \left(\frac{m\pi}{a}\right)}{\left(\left(\frac{m\pi}{a}\right)^2 + \left(\frac{n\pi}{a}\right)^2\right)^2} \cos \frac{m\pi x}{a} \cos \frac{m\pi y}{a}$$
(13c)

$$\sigma_{x} = \frac{E(z)}{1 - v^{2}} \frac{E_{11} + z}{F_{11}} \sum \sum F_{mn} \frac{\left(\frac{m\pi}{a}\right)^{2} + v\left(\frac{n\pi}{a}\right)^{2}}{\left(\left(\frac{m\pi}{a}\right)^{2} + \left(\frac{n\pi}{a}\right)^{2}\right)^{2}} \sin\frac{m\pi x}{a} \sin\frac{m\pi y}{a}$$
(13d)

$$\sigma_{y} = \frac{E(z)}{1 - v^{2}} \frac{E_{11} + z}{F_{11}} \sum \sum F_{mn} \frac{\left(\frac{n\pi}{a}\right)^{2} + v\left(\frac{m\pi}{a}\right)^{2}}{\left(\left(\frac{m\pi}{a}\right)^{2} + \left(\frac{n\pi}{a}\right)^{2}\right)^{2}} \sin\frac{m\pi x}{a} \sin\frac{m\pi y}{a}$$
(13e)

$$\tau_{xy} = \frac{-E(z)}{1+\nu} \frac{E_{11} + z}{F_{11}} \sum \sum F_{mn} \frac{\left(\frac{m\pi}{a}\right) \left(\frac{n\pi}{a}\right)}{\left(\left(\frac{m\pi}{a}\right)^2 + \left(\frac{n\pi}{a}\right)^2\right)^2} \cos\frac{m\pi x}{a} \cos\frac{m\pi y}{a}$$
(13f)

## State II- Gradient distribution in length direction

Consider the rectangular FGM plate-Fig. 2- similar to state 1 while the Young's moduli vary in length direction based on Eq. (14).

**Figure 2.** The distribution of volume fraction **X** direction :  $V_i(x) = (\frac{x}{a})^n$ 

For this case, the coefficients become:

$$A_{11} = \int_{-h/2}^{h/2} \frac{E(x)}{1 - v^2} dz = \int_{-h/2}^{h/2} \frac{\left(\frac{x}{a}\right)^n (E_i - E_m) + E_m}{1 - v^2} dz = \frac{h}{1 - v^2} E(x)$$

$$A_{12} = v A_{11} = \frac{vh}{1 - v^2} E(x)$$

$$A_{66} = \frac{1 - v}{2} A_{11} = \frac{1 - v}{2} \frac{h}{1 - v^2} E(x)$$

$$B_{11} = \int_{-h/2}^{h/2} \frac{zE(x)}{1 - v^2} dz = \frac{E(x)}{1 - v^2} \int_{-h/2}^{h/2} z dz = 0$$

$$B_{12} = v B_{11} = 0$$

$$B_{66} = \frac{1 - v}{2} B_{11} = 0$$

$$C_{11} = \int_{-h/2}^{h/2} \frac{z^2 E(x)}{1 - v^2} dz = \frac{E(x)}{1 - v^2} \int_{-h/2}^{h/2} z^2 dz = \frac{h^3}{12(1 - v^2)} E(x)$$

$$C_{12} = v C_{11} = \frac{v h^3}{12(1 - v^2)} E(x)$$

$$C_{66} = \frac{1 - v}{2} C_{11} = \frac{1 - v}{2} \frac{h^3}{12(1 - v^2)} E(x)$$

$$(15c)$$

It can be seen that the axial forces and bending momentum are uncoupled. This phenomenon is different from the state 1. The equilibrium Eq. (6) becomes:

$$C_{11}\left[\frac{\partial^4 w}{\partial x^4} + \frac{\partial^4 w}{\partial y^4} + 2\frac{\partial^4 w}{\partial x^2 \partial y^2}\right] + \frac{\partial C_{11}}{\partial x}\left[2\frac{\partial^3 w}{\partial x \partial y^2} + 2\frac{\partial^3 w}{\partial x^3}\right] + \frac{\partial^2 C_{11}}{\partial x^2}\left[\frac{\partial^2 w}{\partial x^2} + \nu\frac{\partial^2 w}{\partial y^2}\right] = F$$
 (16)

In order to satisfy the equilibrium equation and boundary conditions, the deflection function w of FGM plate should be the form of:

$$w(x,y) = \sum \sum w_{mn} \sin \frac{m\pi x}{a} \sin \frac{m\pi y}{a}$$
 (17)

By substituting in the equilibrium equation we can find  $w_{mn}$ :

$$\begin{cases}
C_{11} \left[ \left( \frac{m\pi}{a} \right)^2 + \left( \frac{n\pi}{a} \right)^2 \right]^2 + \frac{\partial^2 C_{11}}{\partial x^2} \left[ \left( \frac{m\pi}{a} \right)^2 + \nu \left( \frac{n\pi}{a} \right)^2 \right] \end{cases} w_{mn} = F_0$$

$$w_{mn} = \frac{F_0}{C_{11} \left[ \left( \frac{m\pi}{a} \right)^2 + \left( \frac{n\pi}{a} \right)^2 \right]^2 + \frac{\partial^2 C_{11}}{\partial x^2} \left[ \left( \frac{m\pi}{a} \right)^2 + \nu \left( \frac{n\pi}{a} \right)^2 \right]}$$

So, the stress and strain become:

$$\varepsilon_{x} = -z \frac{\partial^{2} w}{\partial x^{2}} \tag{18a}$$

$$\varepsilon_{y} = -z \frac{\partial^{2} w}{\partial y^{2}} = z \sum \sum \frac{\left(\frac{n\pi}{a}\right)^{2} F_{0}}{C_{11} \left[\left(\frac{m\pi}{a}\right)^{2} + \left(\frac{n\pi}{a}\right)^{2}\right]^{2} + \frac{\partial^{2} C_{11}}{\partial x^{2}} \left[\left(\frac{m\pi}{a}\right)^{2} + \nu \left(\frac{n\pi}{a}\right)^{2}\right] \sin \frac{m\pi x}{a} \sin \frac{n\pi y}{a}}$$
(18b)

$$\gamma_{xy} = -2z \sum \sum \frac{\left(\frac{m\pi}{a}\right) \left(\frac{n\pi}{a}\right) F_0}{C_{11} \left[\left(\frac{m\pi}{a}\right)^2 + \left(\frac{n\pi}{a}\right)^2\right]^2 + \frac{\partial^2 C_{11}}{\partial x^2} \left[\left(\frac{m\pi}{a}\right)^2 + \nu \left(\frac{n\pi}{a}\right)^2\right]} \cos \frac{m\pi x}{a} \cos \frac{n\pi y}{a}$$
(18c)

where

$$\frac{\partial^{2}w}{\partial x^{2}} = \sum \sum \left[ \left( \lambda^{(2)} - \lambda \left( \frac{m\pi}{a} \right)^{2} \right) \sin \frac{m\pi x}{a} \sin \frac{n\pi y}{a} + 2\lambda^{(1)} \left( \frac{m\pi}{a} \right) \cos \frac{m\pi x}{a} \sin \frac{n\pi y}{a} \right) \right]$$

$$\lambda = \frac{16F_{0}}{\pi^{2}} \cdot \frac{1}{C_{11}mn \frac{\pi^{4}}{a^{4}} (m^{2} + n^{2})^{2} + \frac{\partial^{2}C_{11}}{\partial x^{2}} mn \frac{\pi^{2}}{a^{2}} (m^{2} + vn^{2})}{a^{2}} \right]$$

$$\lambda^{(1)} = -\frac{16F_{0}}{\pi^{2}} \cdot \frac{\partial C_{11}}{\partial x} mn \frac{\pi^{4}}{a^{4}} (m^{2} + n^{2})^{2} + \frac{\partial^{2}C_{11}}{\partial x^{2}} mn \frac{\pi^{2}}{a^{2}} (m^{2} + vn^{2})}{a^{2}} \left( C_{11}mn \frac{\pi^{4}}{a^{4}} (m^{2} + n^{2})^{2} + \frac{\partial^{2}C_{11}}{\partial x^{2}} mn \frac{\pi^{2}}{a^{2}} (m^{2} + vn^{2}) \right)^{2}$$

$$\left[ \frac{\partial^{2}C_{11}}{\partial x^{2}} mn \frac{\pi^{4}}{a^{4}} (m^{2} + n^{2})^{2} + \frac{\partial^{4}C_{11}}{\partial x^{4}} mn \frac{\pi^{2}}{a^{2}} (m^{2} + vn^{2}) \right] \cdot \left( C_{11}mn \frac{\pi^{4}}{a^{4}} (m^{2} + n^{2})^{2} + \frac{\partial^{2}C_{11}}{\partial x^{2}} mn \frac{\pi^{2}}{a^{2}} (m^{2} + vn^{2}) \right)^{4}$$

$$\left[ \frac{2\left( \frac{\partial^{2}C_{11}}{\partial x} mn \frac{\pi^{4}}{a^{4}} (m^{2} + n^{2})^{2} + \frac{\partial^{3}C_{11}}{\partial x^{3}} mn \frac{\pi^{2}}{a^{2}} (m^{2} + vn^{2}) \right] \cdot \left( C_{11}mn \frac{\pi^{4}}{a^{4}} (m^{2} + n^{2})^{2} + \frac{\partial^{2}C_{11}}{\partial x^{2}} mn \frac{\pi^{2}}{a^{2}} (m^{2} + vn^{2}) \right)^{4}$$

$$C_{11}mn \frac{\pi^{4}}{a^{4}} (m^{2} + n^{2})^{2} + \frac{\partial^{2}C_{11}}{\partial x^{2}} mn \frac{\pi^{2}}{a^{2}} (m^{2} + vn^{2}) \right] \cdot \left( C_{11}mn \frac{\pi^{4}}{a^{4}} (m^{2} + n^{2})^{2} + \frac{\partial^{2}C_{11}}{\partial x^{2}} mn \frac{\pi^{2}}{a^{2}} (m^{2} + vn^{2}) \right)^{4}$$

$$C_{11}mn \frac{\pi^{4}}{a^{4}} (m^{2} + n^{2})^{2} + \frac{\partial^{2}C_{11}}{\partial x^{2}} mn \frac{\pi^{2}}{a^{2}} (m^{2} + vn^{2}) \right)^{4}$$

$$C_{11}mn \frac{\pi^{4}}{a^{4}} (m^{2} + n^{2})^{2} + \frac{\partial^{2}C_{11}}{\partial x^{2}} mn \frac{\pi^{2}}{a^{2}} (m^{2} + vn^{2}) \right]^{4}$$

$$C_{12}mn \frac{\pi^{4}}{a^{4}} (m^{2} + n^{2})^{2} + \frac{\partial^{2}C_{11}}{\partial x^{2}} mn \frac{\pi^{2}}{a^{2}} (m^{2} + vn^{2}) \right]^{4}$$

$$C_{12}mn \frac{\pi^{4}}{a^{4}} (m^{2} + n^{2})^{2} + \frac{\partial^{2}C_{11}}{\partial x^{2}} mn \frac{\pi^{2}}{a^{2}} (m^{2} + vn^{2}) \right]^{4}$$

$$C_{13}mn \frac{\pi^{4}}{a^{4}} (m^{2} + n^{2})^{2} + \frac{\partial^{2}C_{11}}{\partial x^{2}} mn \frac{\pi^{2}}{a^{2}} (m^{2} + vn^{2})^{2}$$

$$C_{13}mn \frac{\pi^{4}}{a^{4}} (m^{2} + n^{2})^{2} + \frac{\partial^{2}C_{11}}{\partial x^{2}} mn \frac{\pi^{2}}{a^{2}} (m^{2} + vn^{2})$$

$$C_{14}mn \frac{\pi^{4}}{a^$$

$$\tau_{xy} = \frac{E(x)}{1 - v^2} \frac{1 - v}{2} \gamma_{xy}$$
 (20c)

(20b)

## **Finite Element Models**

In the numerical simulation, a square FGM plate with a=50 cm, h=2 cm and material properties of metal and ceramic constituents-Table 1- is considered.

Table 1. material properties

Metal (Ti-6Al-4V) Ceramic 
$$(ZrO_2)$$

$$E_m = 66.2GPa \qquad E_i = 117.0GPa$$

$$v = 0.33 \qquad v = 0.33$$

By applying the n=3,  $F_0 = 1N/cm^2$  and Fourier series coefficient (m= n =20), the theoretical results can be evaluated with numerical modelling. Graded solid elements are implemented by means of direct sampling properties at the Gauss points of the elements. The user material subroutine (UMAT) for modelling of FGM plate with graded elements is provided in ABAUQS.

## **Results**

Fig.3 compares the deflection of the plate with different gradient variation (homogenous plate without variation and variation in Z and X direction, respectively). It can be seen that by applying the higher stiffness material (ceramic) as an inclusion in the metal matrix, the deflection of plate decrease significantly. Moreover, the FGM plate with variation of material constituents in thickness direction has the least maximum deflection with the symmetry parabolic shape. While the maximum deflection for FGM plate with X variation does not occur in the middle of the length. It happens in 0.4 times length.

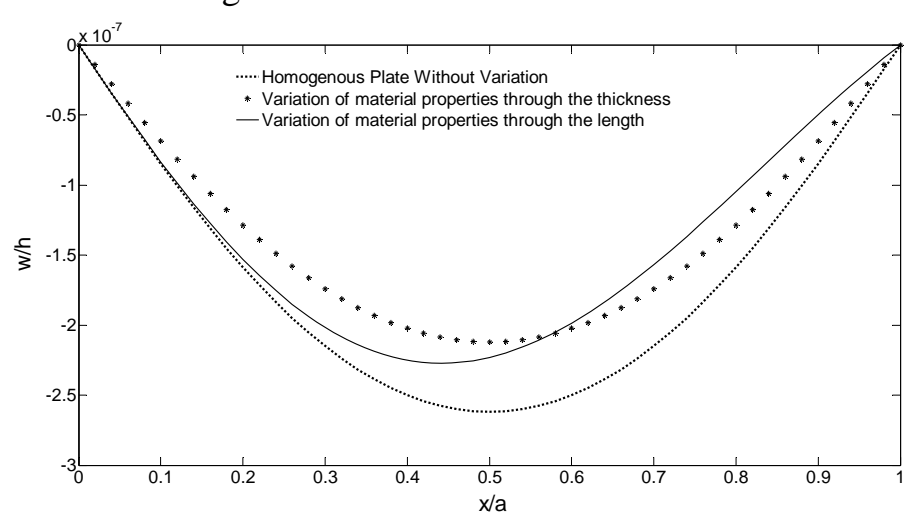


Figure 3. The deflection of the plate

Fig. 4 shows the theoretical and FE (both Shell and Solid elements) results for a square homogenous plate without variation. As revealed in Fig. 4, a good agreement is obtained in using solid elements with mesh size 0.25 with shell elements. So, the

solid elements can be used for modelling of a thin FGM plate instead of shell elements.

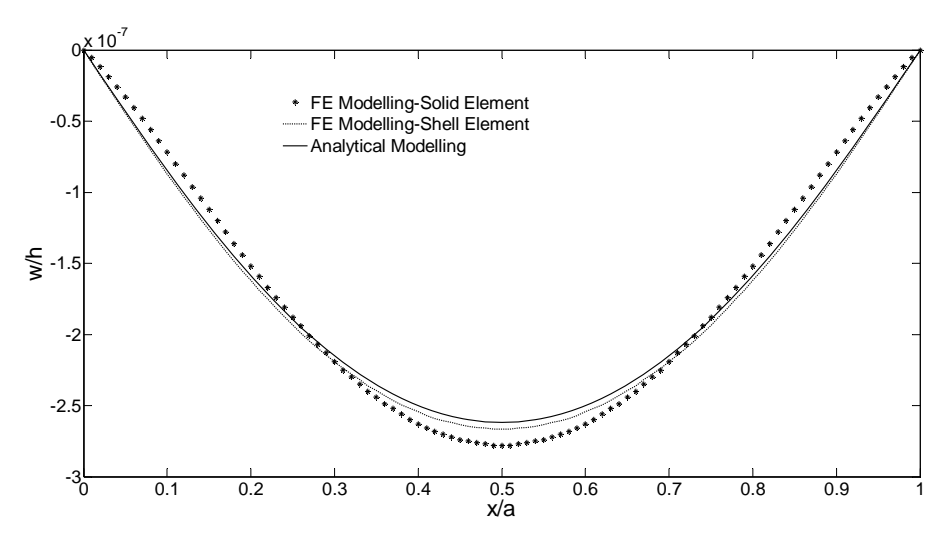


Figure 4. The deflection of the homogenous plate

Figs. 5 and 6 represent the deflection of FGM plate for Z and X gradient variation analytically and numerically, respectively. The analytical and numerical results agree very well in Z and X variation with the maximum error less than 10%. As can be seen from the comparison of two graphs in Fig. 6, the changes between analytical and numerical solution after critical point-maximum deflection- is much pronounced compared to the ones before that. It could be caused by power-law index (n) effect. It can be observed from Fig. 7 that the jump of E occurs at the critical point for n=3 – approximately 0.4 times of plate length-. Indeed, before this point there is a little bit variation in Young modulus and after that the considerable growth of E is obtained. Moreover, as n is raised the jump of E occurs in near the end of the plate (x=a).

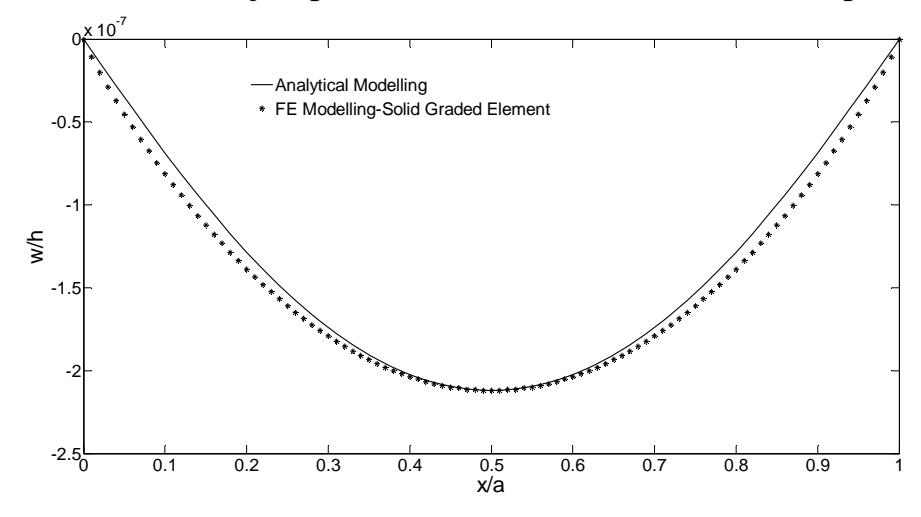


Figure 5. The deflection of the FGM plate with variation of material properties through the thickness

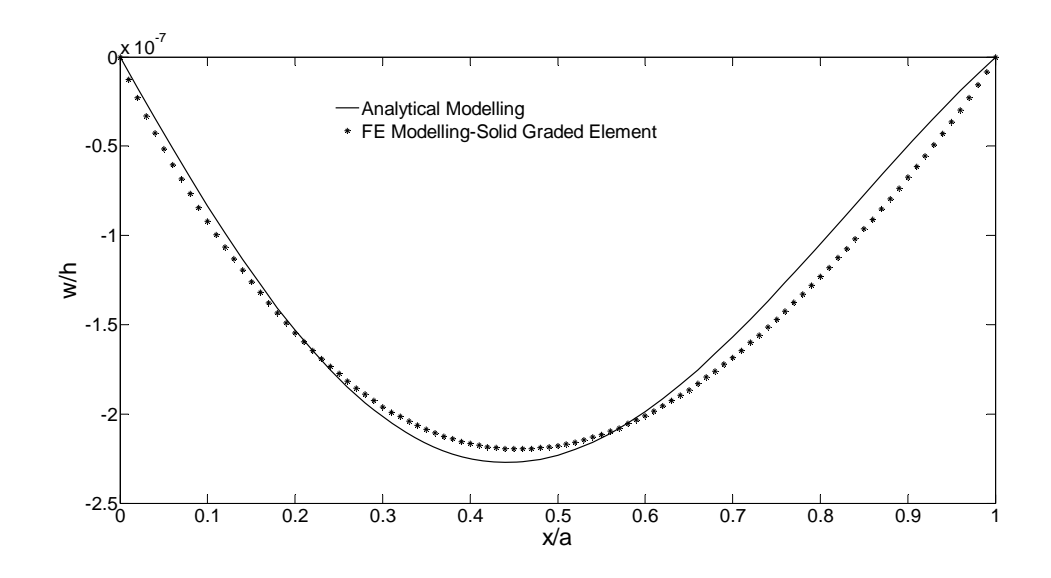


Figure 6. The deflection of the FGM plate with variation of material properties through the length

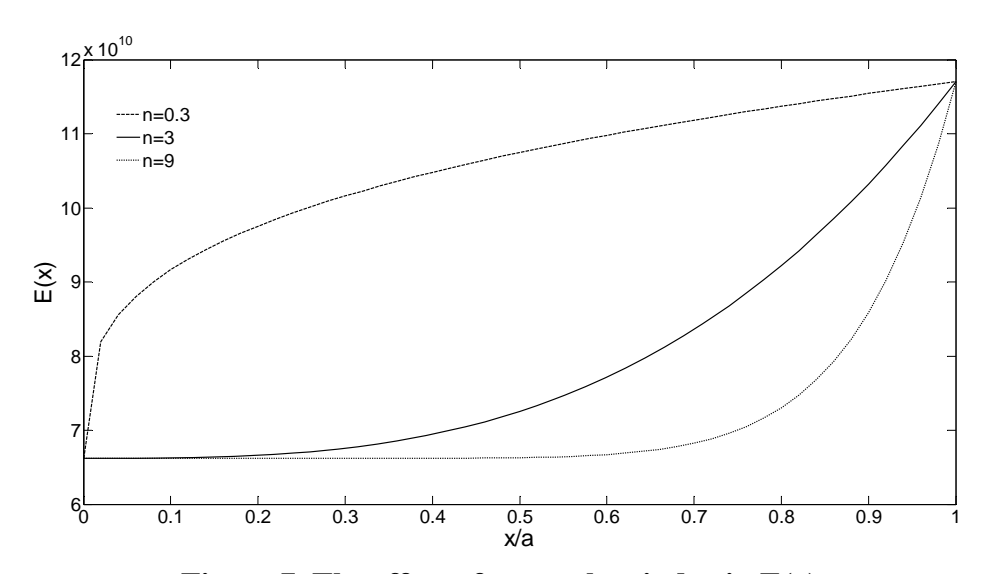


Figure 7. The effect of power-law index in E(x)

The variation of the stress in x direction at the center of the FGM plate along the thickness for state I and II is depicted in Figs. 8 and 9. The stress for FGM plate with Z gradient variation is a function of Z of order 4. This phenomenon coincides with the analytical formulation in Eq. (13d), in which the stresses are proportional to z.E(z). While for X gradient variation, the linear function of Z is presented (based on Eq. (20a)). The maximum tensile and compressive stress in the center of the FGM plate is at the bottom and top edge, respectively. In addition, the good agreement is obtained between analytical and numerical results with the maximum error less than 15%.

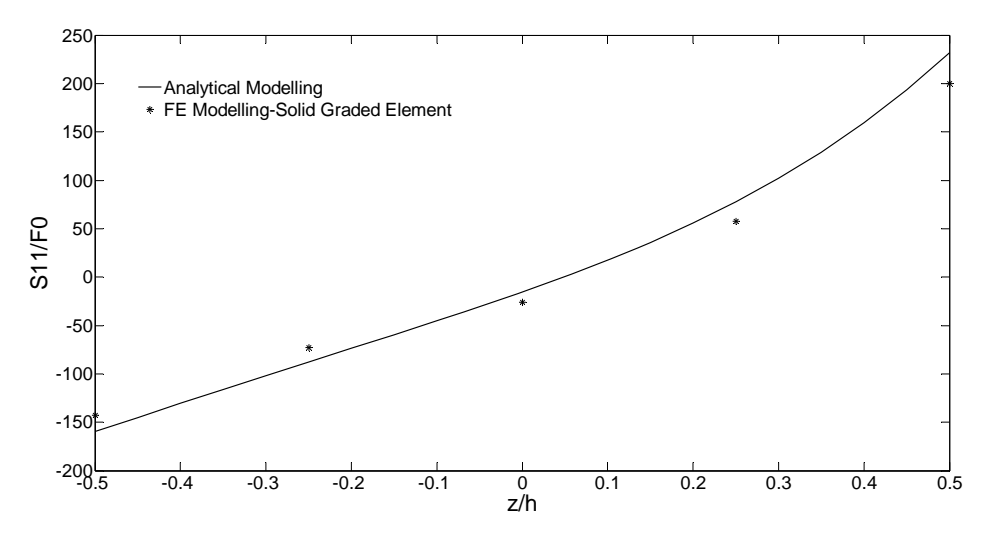


Figure 8. The stress  $\sigma_x$  at the center of FGM plate for variation of material properties through the thickness

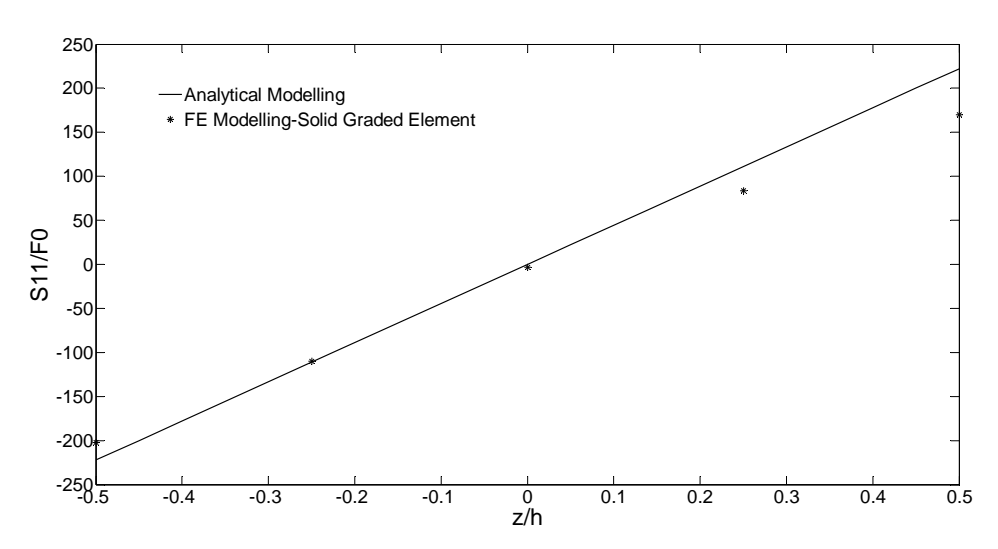


Figure 9. The stress  $\sigma_x$  at the center of FGM plate for variation of material properties through the length

## **Conclusions**

In this study, the theoretical formulation of the simply- supported thin square FGM plate with power-law distribution of volume fraction through the thickness (state I) and length (state II) under transverse loading is derived. The analytical results are also validated by finite element analysis. The FE solution is obtained using solid elements with spatially graded property distribution, which is implemented by a user material subroutine (UMAT) in ABAQUS. The results lead to the following conclusions:

1. Strain at middle surface and deflection for state I are coupled while this phenomenon is different from State II. There is extra coefficient in strain equations in state II that is due to gradient variation in X direction and differentiation of deflection with respect to X.

- 2. Under the assumption of thin plate the theoretical results agree very well with those of FE simulation with solid graded element.
- 3. There is not a linearly proportion between stress and thickness direction in state I. because the Young's moduli of this state are functions of z of order n-power law index-, so the stress indicates a function of z of order n+1.
- 4. The maximum deflection occurs in the middle plate for sate I while it happens before that in state II-at nearby 0.4 times of length-.

The approach outlined in this paper would be beneficial for the ideal FGM plate which variation of volume fraction of constituents is controlled and obey a specific function of distribution. This aim could be achieve with aid of 3D printing that can control local composition and microstructure.

## References

- Akbarzadeh, A. H., Hosseini zad, S. K., Eslami, M. R., & Sadighi, M. (2010). Mechanical behaviour of functionally graded plates under static and dynamic loading. *Proceedings of the Institution of Mechanical Engineers, Part C: Journal of Mechanical Engineering Science*, 1(-1), 1-8.
- Bocciarelli, M., Bolzon, G., & Maier, G. (2008). A constitutive model of metal–ceramic functionally graded material behavior: Formulation and parameter identification. *Computational Materials Science*, 43(1), 16-26.
- Cheng, Z. Q., & Batra, R. C. (2000). Exact Correspondence between Eigenvalues of Membranes and Functionally Graded Simply Supported Polygonal Plates. *Journal of Sound and Vibration*, 229(4), 879-895.
- Chi, S.-H., & Chung, Y.-L. (2006). Mechanical behavior of functionally graded material plates under transverse load—Part I: Analysis. *International Journal of Solids and Structures*, 43(13), 3657-3674.
- Eghtesad, A., Shafiei, A. R., & Mahzoon, M. (2012). Study of dynamic behavior of ceramic–metal FGM under high velocity impact conditions using CSPM method. *Applied Mathematical Modelling*, 36(6), 2724-2738.
- El-Desouky, A., Kassegneb, S. K., Moonb, K. S., McKittricke, J., & Morsib, K. (2013). Rapid processing & characterization of micro-scale functionally graded porous materials. *Journal of Materials Processing Technology*, 1251–1257.
- Guo, L., & Noda, N. (2014). Investigation Methods for Thermal Shock Crack Problems of Functionally Graded Materials—Part I: Analytical Method. *Journal of Thermal Stresses*, 37(3), 292-324.
- Kieback, B., Neubrand, A., & Riedel, H. (2003). Processing techniques for functionally graded materials. *Materials Science and Engineering*, A362, 81–105.
- Navazi, H. M., Haddadpour, H., & Rasekh, M. (2006). An analytical solution for nonlinear cylindrical bending of functionally graded plates. *Thin-Walled Structures*, 44(11), 1129-1137.
- Pan, E. (2003). Exact Solution for Functionally Graded Anisotropic Elastic Composite Laminates. *Journal of Composite Materials*, 37(21), 1903-1920
- Sun, D., & Luo, S.-N. (2011). Wave propagation and transient response of functionally graded material circular plates under a point impact load. *Composites Part B: Engineering*, 42(4), 657-665.
- Thai, H.-T., & Choi, D.-H. (2013). Analytical solutions of refined plate theory for bending, buckling and vibration analyses of thick plates. *Applied Mathematical Modelling*, *37*(18-19), 8310-8323.
- Torshizian, M. R., & Kargarnovin, M. H. (2014). The mixed-mode fracture mechanics analysis of an embedded arbitrary oriented crack in a two-dimensional functionally graded material plate. *Archive of Applied Mechanics*, 84(5), 625-637.
- Wang, C., & Xu, X. (2014). A new hybrid element analysis for exponentially varying FGM based on an asymptotic stress field. *Acta Mechanica Solida Sinica*, 27(3), 315-330.
- Wang, Z., Guo, L., & Zhang, L. (2013). A general modelling method for functionally graded materials with an arbitrarily oriented crack. *Philosophical Magazine*, 94(8), 764-791.